THE JOURNAL OF PHYSICAL CHEMISTRY B

ARTICLE

pubs.acs.org/JPCB

Ultrafast Transient Optical Studies of Charge Pair Generation and Recombination in Poly-3-Hexylthiophene(P3ht):[6,6]Phenyl C61 Butyric Methyl Acid Ester (PCBM) Blend Films

James Kirkpatrick,*[,†] Panagiotis E. Keivanidis,[†] Annalisa Bruno,[‡] Fei Ma,[§] Saif A. Haque,[‡] Arkady Yarstev,[§] Villy Sundstrom,[§] and Jenny Nelson*[,†]

[†]Department of Physics, Imperial College London, London SW7 2AZ, United Kingdom

[‡]Department of Chemistry, Imperial College London, London SW7 2AZ, United Kingdom

[§]Department of Chemical Physics, Lund University, P.O. Box 124, SE-22100 Lund, Sweden

Supporting Information

ABSTRACT: Charge generation and recombination are studied in blend films of poly-3-hexylthiophene (P3HT) and [6,6′]phenyl C61 butyric acid methyl ester (PCBM) using ultrafast transient absorption spectroscopy. We find that the charge generation yield depends upon both blend film composition and thermal annealing. The data suggest that recombination occurs over a wide range of time scales and that, in the least favorable cases, the fastest charge recombination occurs on a time scale similar to exciton diffusion. The results are explained using a simple model that incorporates the effect of P3HT domain size on exciton diffusion and uses empirical models of recombination kinetics. We propose our method as a route to interpretation of spectroscopic data where different processes occur on similar time scales.

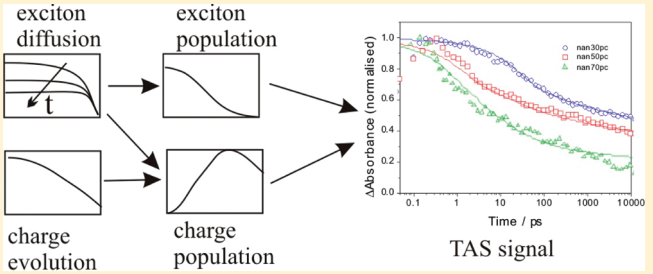

INTRODUCTION

One of the major factors controlling the performance of organic bulk heterojunction solar cells is the yield of free charge pairs that results from the dissociation of a photoinduced exciton.[1] In an agreed picture, generation of a singlet exciton by photon absorption is followed by diffusion and dissociation, or decay, of the exciton, and exciton dissociation results in geminate charge pairs, some of which escape their mutual attraction to contribute to the photocurrent. However, the mechanism of charge pair generation and the factors that control the charge generation efficiency are not yet understood. Disentangling the dynamics of the different processes is difficult because of the effect of disorder on exciton and charge dynamics. Exciton lifetime is influenced by the distance over which excitons may diffuse, i.e., by the size of polymer domains, which depends on processing and blend composition. Recombination of both geminate and nongeminate charges may take place over a range of time scales, resulting from the range of times for charge transfer in an energetically and structurally disordered medium. A model of charge and exciton dynamics should therefore be able to incorporate the effects of structural variations and disorder. Ultrafast transient absorption spectroscopy (TAS) provides a tool to study the dynamics and yield of charge pair generation under different conditions, provided that the transient absorption features can be correctly assigned. TAS can then be used together with a suitable model to investigate the influences of the blend film microstructure on charge generation.

The combination of poly-3-hexylthiophene (P3HT) with [6,6]phenyl C61 butyric acid methyl ester (PCBM) is a material system of particular interest because it has been widely studied for organic solar cell applications and because the charge generation yield is strongly dependent on the blend film composition and on the microstructure, as controlled by thermal annealing.[2] Previous studies have demonstrated the influence of the blend composition and microstructure on charge generation yield as monitored in the microsecond time domain.[2a] Several recent studies have addressed charge generation kinetics;[3] several of them[3a,b,f] conclude that charge generation occurs on multiple time scales, as a consequence of exciton diffusion and that annealing influences the kinetics of charge pair generation.[3a,b] Marsh and co-workers demonstrate that charge recombination also occurs on multiple time scales.[3a] However, no quantitative explanation in terms of the exciton diffusion parameters has yet been presented. Previously, low excitation density TAS has been used to explain the dynamics of charge generation on sub ns time scales in polyfluorene:PCBM blend films[4] and polyfluorene:P3HT blends.[5] Those studies revealed that even at low excitation densities charge recombination was significant on the sub ns time scale and could therefore compete with charge collection. A similar conclusion was reached by

Received: June 18, 2011
Revised: November 12, 2011
Published: November 14, 2011

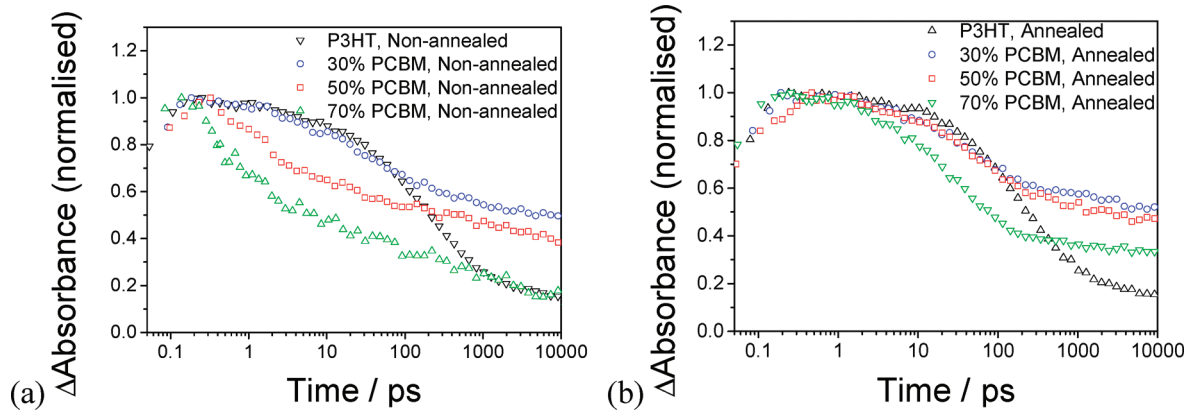

Figure 1. Normalized transient absorbance kinetics at 1000 nm for (a) nonannealed and (b) annealed blend films of different compositions. Films were excited at 550 nm with a power of 20 nJ per pulse.

Howard et al., who studied charge generation in P3HT:PCBM blends before and after annealing.[3f] Here, we apply similar techniques to study charge generation in P3HT:PCBM blend films as a function of blend film composition and of thermal annealing. In contrast to previous studies of charge generation kinetics, we explain the results quantitatively in terms of simple models of exciton diffusion. This procedure leads us to conclude that the observed kinetic data on ps−ns time scales are largely consistent with a mechanism dominated by exciton diffusion. We also deduce that, at least in the least favorable cases of high PCBM loading and no annealing, charge recombination can occur on a similar time scale to that of charge generation following exciton diffusion.

RESULTS AND DISCUSSION

We measured transient absorption (TA) dynamics for three composition ratios (30, 50, and 70 wt % PCBM) where the blend film microstructure is known to be significantly different. In order to ensure that the excitation density was low enough to avoid nonlinear effects, the fast (0−100 ps) dynamics were first analyzed as a function of laser intensity, for the untreated and annealed films of pristine P3HT and of the P3HT:PCBM 50 wt % blends. For these systems, the shape of the normalized kinetic trace (normalized by setting the time at which the signal reaches half its maximum value to $t = 0$ and to a ΔOD value of 0.5) is invariant at excitation densities less than 20 nJ pulse^{-1} (5.68 μJ cm^{-2}), indicating that nonlinear effects are not significant at these intensities (see Figure SI1, Supporting Information). Subsequently, an excitation density (obtained by assuming that all films have an optical density of 0.5 and that generation is uniform throughout a cylinder of film with an area of 3.52 × 10^{-3} cm^2 and thickness of 500 nm) of 20 nJ/pulse was used. This corresponds approximately to a volume generation rate of 8 × 10^{17} cm^{-3}, comparable to solar excitation densities.

Figure 1 shows the normalized TA decay traces for films of pristine P3HT and all three blend ratios, for nonannealed (a) and annealed (b) films. The traces for the pristine polymer are approximately exponential with a lifetime of ∼200 ps. The traces for all blend films are multiphasic showing a fast phase, which in the case of annealed blend films has a similar time constant to the pure polymer, and a slow phase, which follows an approximate power law. Previous transient absorption studies of P3HT:PCBM blend films in the ns−ms domain showed that the hole polarons in P3HT decayed like a power law,[6] likely as a result of diffusion limited recombination involving a distribution of trap states.[7] Given that both singlet excitons and positive polarons in P3HT are known to absorb at the probe wavelength, we interpret the signal as due to the sum of contributions from excitons (mainly present on ps−ns time scales) and positive polarons (mainly present on ns and longer time scales). (N.B. negative polarons on PCBM can be neglected as their extinction coefficient is an order of magnitude weaker.[8])

By comparing the traces for the different blend ratios and for the nonannealed and annealed films, we can make several remarks. First, the amplitude of the signal at 10 ns, which can be assigned largely to charges, relative to that at 0.2 ps, due primarily to excitons, increases markedly upon PCBM addition. It is also larger for the 30% than for the 50% and 70 wt % blends. This indicates that charge generation results largely from charge transfer to PCBM and that the yield is influenced by blend film composition and microstructure, in agreement with previous photocurrent and TAS studies.[2a,3b] Second, the decay of the absorbance during the first 1−10 ps, which can be assigned largely to singlet excitons, is generally faster for high than for low PCBM content and is also faster for nonannealed blends than for the same blends when annealed. The reduced exciton lifetime at larger PCBM content may result from smaller P3HT domains, and the reduced lifetime before annealing is consistent with the PCBM being more finely dispersed in the polymer before annealing, resulting is a higher probability of the exciton finding a PCBM site quickly, in agreement with microstructural studies. However, it should be noted that the most rapid exciton decay does not correlate with the highest yield of polarons, as estimated from the signal at 10 ns (or from the signal at 1 μs in ns−ms TAS experiments[2a]). Thus, the process that removes excitons on the ps time scale does not necessarily result in generation of long-lived charges. This suggests that in order to explain the results, we will need to invoke at least one process other than the long-lived charge generation directly following exciton dissociation and that the competition between long-lived charge generation and the competing process is influenced by blend film composition and microstructure. We will interpret this as meaning that some recombination occurs on a time scale comparable to exciton diffusion and hence to charge generation. We also note here that in the case of the 50 wt % and 70 wt % nonannealed blend films, the deactivation process is clearly multiphasic even on time scales less than 100 ps.

In order to find a quantitative explanation for the observations, we develop a simple model of the dynamics of the exciton and polaron populations. We assume that energy migration operates by a normal (not anomalous), 1-D diffusion, and we neglect any other long-range energy transfer processes between separated P3HT domains. Photogenerated excitons can decay either radiatively or nonradiatively; those excitons that reach the P3HT:PCBM domain boundary before decaying generate a bound charge pair immediately and with unit efficiency. This is equivalent to assuming that the exciton density $X(t,x)$ obeys the following partial differential equation and absorbing boundary conditions:[9]

$$\frac{\partial X}{\partial t} = D\frac{\partial^2 X}{\partial x^2} - \frac{X}{\tau_r} \qquad X(t,0) = X(t,L) = 0 \tag{1}$$

where D is the exciton diffusion coefficient, τ_r is the time constant for the exciton decay, and L is the linear size of the polymer domain. The total exciton population per photon absorbed $\xi(t)$ is found by integrating the exciton density $X(t,x)$ over x and is 1 at $t = 0$. Integrating the diffusion term over space also gives the rate of creation of charges $\gamma(t)$. In the Supporting Information, we include the analytic solution to eq 1 for a uniform initial population of excitons and the resulting forms of $\gamma(t)$ and $\xi(t)$.

In order to determine the total charge population $P(t)$, it is necessary to know the dynamics for a charge pair $p(t)$ generated at $t = 0$. This problem has been addressed using a detailed Monte Carlo simulation. Such methods have been used to simulate μs−ms bimolecular recombination dynamics[7,10] and to model the competition of geminate recombination and charge generation[11] in polymer/fullerene blend films. Some of these studies showed that the observed power-law decay of polaron population could be explained by polaron diffusion through an energetic distribution of trap states, such that the exponential tail of the trap distribution determines the critical exponent of the power law decay.[7] Simulations of geminate recombination in ref 11 showed that those charges that escape geminate recombination then follow a power law decay. We take advantage of these findings to use a power-law form for the bimolecular recombination of charges and apply it to those charges that escape geminate recombination.

Geminate recombination may also be expected to occur over a range of time scales, given that the rate of recombination will depend on the relative position and orientation of the molecular units involved and on their local environment, and these factors will be varied in a disordered blend film. (In polymer blend films, for example, the molecular orientation is known to influence charge generation and exciton dynamics.[12]) To allow for such dispersive dynamics while minimizing the number of fitting parameters, we choose to treat geminate recombination as an exponential process in those cases where this approximation represents the data and to use a power law decay in other cases. The choice of a power law is again motivated by the evidence for exponential tails of states in some molecular semiconductors[7,13] and previous arguments that power law luminescence behavior at short times can result from geminate recombination in disordered systems.[14] However, we stress that we cannot, on the basis of the results in this article, infer the form of the geminate recombination dynamics uniquely. Other forms such as a distribution of rates resulting from a normal distribution of site energies or of site separations could also, in principle, be applied. The point is rather that in some of the cases studied here, dispersive dynamics must be used to describe the geminate recombination dynamics.

We therefore use the following empirical formula for $p(t)$ at high P3HT content and for the annealed films:

$$p(t) = \exp\left(\frac{-\tau_b}{\tau_g}\right)\exp\left(\frac{{\tau_b}^2}{t\tau_g + \tau_b\tau_g}\right)\left(1 + \frac{t}{\tau_b}\right)^{-\alpha} \tag{2}$$

This expression represents competition between geminate recombination, which occurs on short times ($t < \tau_b$) and is modeled by an exponential with a time constant τ_g and a dispersive nongeminate recombination process that takes over at longer times ($t > \tau_b$) and produces a power-law decay with exponent α. Note that the prefactor $\exp(-\tau_b/\tau_g)$ is the fraction of charges, which escapes geminate recombination and as such represents the branching ratio between geminate recombination and spatial separation of an initially formed bound charge pair. The separated charges may then contribute to nongeminate recombination. The parameter τ_b may be regarded as the time scale for the initial separation of charges via hopping, to bring them outside the spatial range in which geminate recombination dominates. A more detailed justification for the choice of this equation is given in the Supporting Information.

In the case of nonannealed high PCBM content (50 and 70 wt %) blend films, the early stage of the kinetic trace shows a power law character even at short times. This suggests that for those samples a characteristic time scale for geminate recombination does not exist, and we therefore use a power law model for geminate recombination to fit these data, as explained above. In these cases, we use the following empirical function to model $p(t)$:

$$p(t) = \left(1 + \frac{t}{\tau_d}\right)^{-\alpha_d}\left(1 + \frac{t}{\tau_b}\right)^{-(\alpha - \alpha_d)} \tag{3}$$

This expression tends to a constant at times shorter than τ_d and to a power law decay with exponent α at long times, with a second power law regime (exponent α_d) at intermediate times.

The number of charges per absorbed photon $P(t)$ is then obtained by convolving the rate $\gamma(t)$ with the temporal evolution $p(t)$

$$P(t) = \int_{TMIN}^{t} \gamma(t')p(t - t')\mathrm{d}t' \tag{4}$$

Finally, the populations of excitons ξ and polarons P are weighted with the appropriate extinction coefficients and summed together to obtain a model for the normalized observed transient absorbance. When the transient absorbance data are normalized as described above, the resulting quantity effectively represents the transient absorbance per absorbed photon divided by the exciton extinction coefficient at 1000 nm, if we can assume that each absorbed photon generates one P3HT exciton at $t = 0$. Then, the normalized absorbance can be expressed as

$$\Delta A(t) = \xi(t) + \varepsilon_{rel}P(t) \tag{5}$$

where ε_{rel} is the ratio of the polaron extinction coefficient at 1000 nm to that of the exciton.

Of the parameters required by the model, the exciton lifetime τ_r can be estimated to be 200 ps by fitting the absorbance decay for pristine P3HT; the exciton diffusion length L_{ex} is taken as 5 nm, according to literature reports,[15] which corresponds to a

diffusion constant of $D = 0.125$ nm^2/ps. Note that the value of the parameters obtained are not sensitive to the diffusion constant. Changing D would simply change the exciton diffusion length and scale all the lengths accordingly. Of the remaining five parameters, the relative extinction coefficient of charges with respect to excitons at 1000 nm, ε_{rel}, the exponents for the power law decay, α, and the nongeminate pair initial lifetime, τ_b, will be the same for all cases studied. The decision to keep τ_b and α fixed is motivated by the fact that trap-limited bimolecular recombination is influenced mainly by disorder within the bulk of the different domains rather than by the interfacial regions, and these pure domains should be less influenced by composition and processing, as well as by the observation that the long time power law decay follows similar dynamics in all cases. The remaining case specific parameters are τ_g and L for the case of the exponential geminate recombination and L, α_d, and τ_d for the case of the power-law geminate recombination. We let L vary to account for the expected variation in polymer domain size with blend composition and processing. The parameters τ_g, α_d, and τ_d are allowed to vary to account for possible variations in the interfacial environment in the different films.

The kinetic traces for all six blend films studied are fit by varying the parameters subject to the constraints given previously. The fitted parameters are listed in Tables 1 (global parameters) and 2 (case specific parameters). Figure 2 shows an analysis of the fit for the nonannealed and annealed 50 wt % blend films. Fits for all cases studied are included in Supporting Information, Figure SI2. The solid and dashed curves depict the evolution of the populations of excitons and charges in the system, respectively. The exciton population decays exponentially, whereas the charge populations initially increase exponentially due to generation but then fall due to the two recombination mechanisms. The time scale for the decay in exciton population and rise in charge population is determined in our fitting procedure by the polymer domain size, L. We point out here that the observed power law behavior at long times can only be obtained if the branching between pathways that lead to nongeminate and geminate recombination occurs at very short times. One mechanism for such fast branching is the dynamic competition between the separation and thermalization of a vibrationally hot geminate pair. If geminate charges fail to escape their mutual Coulomb attraction during thermalization, they will be committed to recombine geminately; otherwise, they will be free to contribute to current or recombine by a bimolecular process.[16] Another explanation for early branching could be that excitons dissociate in sites of different molecular and dielectric environments, some of which facilitate rapid charge separation, while others do not.

Figure 3 shows fits to the decay traces for all annealed and nonannealed films. In order to reproduce the amplitude of the transient absorbance at 1−10 ns relative to the initial peak absorbance and to fit the shape of the initial kinetic decay, it was necessary to vary both the domain size L and the geminate recombination parameters for the different cases. The fitted value of L tends to decrease with increasing PCBM content and is larger for annealed than nonannealed films. This is consistent with the decreasing fraction of P3HT in the blend film as PCBM content increases and with the observation that PCBM molecules aggregate during thermal annealing to leave larger P3HT domains.[2a,17] Both of these trends are supported by measurements of photoluminescence quenching reported previously,[2a] which consistently show (i) decreasing PL intensity with increasing PCBM content in nonannealed films, indicating that dispersed PCBM molecules act as quenching sites for excitons in P3HT, and (ii) weaker PL from nonannealed than annealed films, indicating smaller or less pure P3HT domains before annealing induced phase segregation. A much smaller value of L is needed to fit the 70% PCBM annealed blend data than the 30% or 50% annealed blends, in order to account for the faster kinetics at short times in the 70% PCBM case. (The parameter L strongly influences short time kinetics since it controls the

Table 1. Global Fit Parameters

parameter	value
L_{ex} (nm)	5.0
ε_{rel}	0.8
α	0.05
τ_b (ps)	100

Table 2. Case Specific Fit Parameters

	L (nm)	τ_g (ps)	τ_g (ps)	α_d	exp($-\tau_b/\tau_g$)
annealed 30 wt %	5.3	600			0.85
annealed 50 wt %	6.5	600			0.85
annealed 70 wt %	2.5	135			0.48
nonannealed 30 wt %	5.5	600			0.85
nonannealed 50 wt %	1.0		1.0	0.10	
nonannealed 70 wt %	0.7		1.0	0.22	

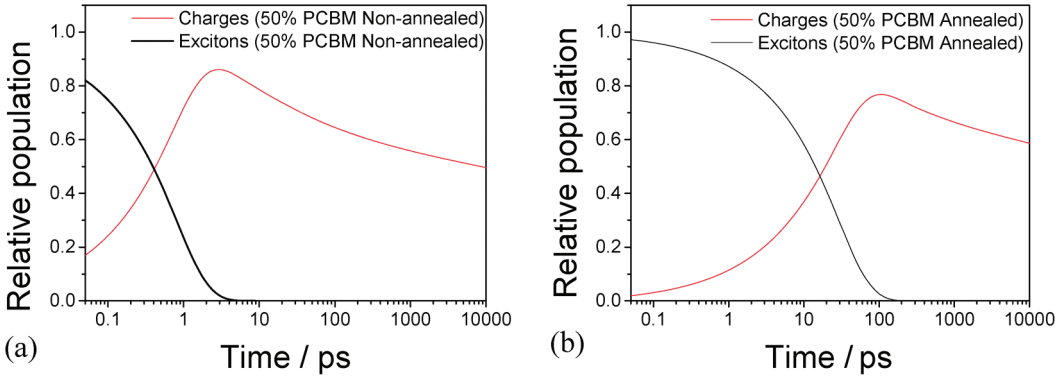

Figure 2. Exciton (black, solid line) and charge (red, dashed line) populations for the fits of the kinetics for the (a) nonannealed and (b) annealed blend films containing 50 wt % PCBM. Fitting parameters are listed in Tables 1 and 2.

dx.doi.org/10.1021/jp205731f |J. Phys. Chem. B 2011, 115, 15174–15180

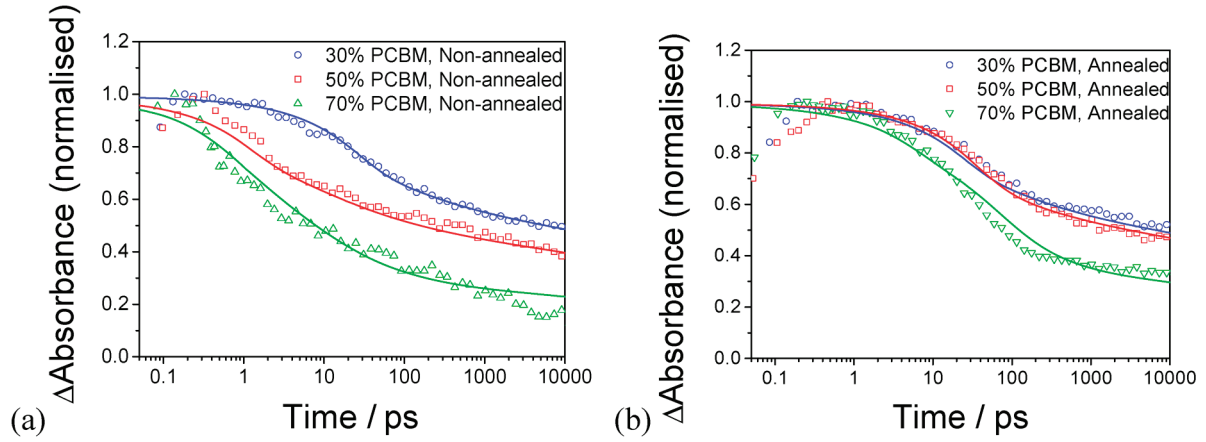

Figure 3. Fits for the (a) nonannealed and (b) annealed blend films. Fits are obtained using eq 1 together with eq 2 for $p(t)$ for all annealed films and the 30% PCBM nonannealed film, and with eq 3 for $p(t)$ in the other cases. Fitting parameters are shown in Tables 1 and 2.

exciton diffusion time.) A smaller P3HT domain size for high PCBM content films is compatible with the eutectic phase behavior of this blend system, where blends with high PCBM content are expected to contain aggregates of PCBM within a matrix of the two components, while low PCBM content blend films contain larger crystallites of P3HT.[18] The P3HT domain size is expected to be much smaller for the PCBM rich, hypoeutectic blend films than for eutectic or PCBM poor films containing pure P3HT crystallites. In the case of the nonannealed films, the much smaller values of L needed for the two higher PCBM content blends indicate the lack of large P3HT crystallites in these two cases, as supported also by spectroscopic data previously reported.[2a] The dominant effect of L on the dynamics is evidenced in the Supporting Information, Figure SI2, which shows more rapid exciton decay, and consequently faster signal decay at short times, in cases with a shorter L. This figure also shows how the results of fits using eq 2 and eq 3 are qualitatively similar, such that the three nonannealed cases follow a clear trend that is consistent with the trend in the fitted values of the domain size.

The need to use a dispersive geminate recombination model at high PCBM content for nonannealed cases suggests that these films are relatively disordered and contain a larger number of molecularly dispersed PCBM molecules. Such molecules would introduce dissociation sites where geminate recombination is unavoidable and thus increase the probability of fast geminate recombination events, as well as extending the range of time scales for geminate recombination. Another possible explanation is that in the annealed films, slower geminate recombination events do not occur because pairs that would have a slow geminate recombination time separate before geminate recombination occurs. Whatever the mechanism, it is clear from the data that there is a process that operates on a time scale competitive with the exciton lifetime and removes excitons without generating longer lived polarons. In our model, that removal process is assumed to be geminate recombination. The fraction of charges escaping geminate recombination is listed in Table 2 for those cases that could be fit with eq 2.

The transient optical data shown here reveal some significant differences when compared to measurements taken on the μs−ms time scale. First, the decays of charge densities are weak compared to the more pronounced power law decays seen on the μs time scale.[2a,6a] Second, the dependence of the charge generation yield in annealed films is rather different, with the largest yield seen here for 30 wt % PCBM blend films, while in the μs regime transient, absorption is usually maximized at larger PCBM contents of 40−50 wt %, consistent with the maximum photocurrent.[2a] These discrepancies indicate that different charge recombination mechanisms may be operating in the nanosecond and micromillisecond domains although the origin of these differences is still not clear.

In contrast with previous work, we have shown that transient absorption kinetic data for P3HT:PCBM blend films is consistent with a simple model of exciton diffusion. By analysis of the shape of the transients in the ps−ns time range, we conclude that recombination may be significant in the nanosecond time range even for annealed films, in partial contrast with previous studies.[3a,b] The trends in fitting parameters with a blend ratio or film treatment can be convincingly correlated to changes in microstructure: blends with lower PCBM content tend to contain larger P3HT domains, while annealed films contain larger P3HT domains than nonannealed films and are generally more ordered (exponential geminate recombination). However, it should be noted that changes in domain shape due to annealing would not be captured by our simple one-dimensional model.

The observation of rapid recombination of photogenerated charges in the films studied here raises the question of whether the same loss pathways will be operational in a device, where an electric field may be present due to the different electrochemical potential of the electrodes. Preliminary measurements using the electromodulated differential absorption technique on devices made from similarly processed films suggest that for this material system kinetics are barely affected by the field present at open circuit.[19] However, the topic clearly merits further discussion, and the situation for different material systems may well be different.

CONCLUSIONS

In conclusion, we have used ultrafast measurements of transient absorption and a simple model to study the kinetics of the charge generation in P3HT:PCBM blend films as a function of microstructure, as controlled both by composition and annealing. We find that microstructure influences charge generation through both the size of the pure polymer domains through which excitons diffuse before dissociation and the environment

in which the exciton dissociates, which determines the competition between fast (exponential and geminate) and slow (nongeminate and power law) recombination. We find that polymer domains are larger for annealed than nonannealed blends and for lower than higher PCBM content blends, in agreement with previous optical and structural measurements. Smaller polymer domains tend to lead to faster generation and faster recombination of charges, with the net result of fewer long-lived charges than that for larger domains. We also find that dispersive recombination kinetics must be allowed for in the case of the most disordered, PCBM rich films, suggesting that the interfacial regions are very disordered in those cases. Although the detailed relationship between the local nanostructure and the fate of geminate pairs is unclear, it seems that more finely intermixed morphologies lead to a faster decay of charges. Finally, it should be noted that the fastest, geminate recombination events occurs on time scales that are similar to the natural exciton decay. Our findings are in broad agreement with the recent results of Howard et al.[3f] To maximize the generation of long-lived charges, blend film microstructure should be controlled to minimize such fast geminate losses. Various routes to the control of the film microstructure have been proposed, including choice of solvent,[20] use of additives,[21] and through the use of multiblock macromolecules to form structures of controlled dimension.[22]

EXPERIMENTAL DETAILS

P3HT and PCBM materials were obtained from Merck and from Solenne, respectively, and were used without further purification. All blend films were spin-cast from chlorobenzene solutions of 15 mg/mL concentration. Appropriate P3HT:PCBM mass ratios were chosen for obtaining PCBM loadings of 0 wt %, 30 wt %, 50 wt %, and 70 wt %. All fabricated films were deposited on quartz substrates by spin coating in ambient conditions. To study the effect of thermal annealing, a second set of films was prepared in identical fashion, and it was annealed in a N_2 filled glovebox. The films were left on a hot plate at 140 °C for 30 min, and they were rapidly quenched upon their transfer on a cold metal surface. All films were encapsulated by attaching glass slides of ~1 mm thickness onto the photoactive layer side of the films by degassed epoxy.[23] Effective protection of the sample by this encapsulation was found to be essential to prevent photodegradation of the sample in air. Nonencapsulated samples were found to display different transient absorption kinetics after repeated exposure to the excitation source.

TAS studies with 30 fs pulses were carried out using an experimental setup based on a commercial 1 kHz Clark MXR CPA 2001 laser, pumping a noncollinear optical amplifier (Clark MXR Inc. NOPA) to generate the probe pulses. Another amplifier (TOPAS white light conversion) was used to generate probe pulses at 550 nm. TA kinetics were measured by the detection of undispersed probe and reference pulses. More information can be found in ref 4. Films were excited at 550 nm, near the peak of the P3HT absorption, with an excitation power of 20 nJ/pulse for all the data presented and focused on a spot of 3.52×10^{-3} cm^2. The probe wavelength was set to 1000 nm where the spectrum of the positive P3HT polaron is known to have a maximum[6a] corresponding to the absorption of localized polarons in disordered domains of the polymer.[3b]

ASSOCIATED CONTENT

Supporting Information. Intensity dependence of transient absorption kinetics, fitted charge and exciton population kinetics in all cases, solution of the diffusion equation, and a derivation of eq 2. This material is available free of charge via the Internet at http://pubs.acs.org.

AUTHOR INFORMATION

Corresponding Author

*E-mail: kirkpatrick@maths.ox.ac.uk (J.K.); jenny.nelson@imperial.ac.uk (J.N.).

ACKNOWLEDGMENT

J.K. acknowledges the EPSRC for financial support. J.N. acknowledges the support of EPSRC and the Royal Society. Laser Lab Europe is gratefully acknowledged for the access to experimental facilities in the University of Lund.

REFERENCES

(1) Clarke, T. M.; Ballantyne, A. M.; Shoaee, S.; Soon, Y.; Duffy, W.; Heeney, M.; McCulloch, I.; Nelson, J.; Durrant, J. R. *Adv. Mater.* **2010**, *22* (46), 5287–5291.

(2) (a) Keivanidis, P. E.; Clarke, T. M.; Lilliu, S.; Agostinelli, T.; Macdonald, J. E.; Durrant, J. R.; Bradley, D. D. C.; Nelson, J. *J. Phys. Chem. Lett.* **2010**, *1* (4), 734–738. (b) Veldman, D.; Ipek, O.; Meskers, S. C. J.; Sweelssen, J.; Koetse, M. M.; Veenstra, S. C.; Kroon, J. M.; van Bavel, S. S.; Loos, J.; Janssen, R. A. J. *J. Am. Chem. Soc.* **2008**, *130* (24), 7721–7735.

(3) (a) Marsh, R. A.; Hodgkiss, J. M.; Albert-Seifried, S.; Friend, R. H. *Nano Lett.* **2010**, *10* (3), 923–930. (b) Guo, J. M.; Ohkita, H.; Benten, H.; Ito, S. *J. Am. Chem. Soc.* **2010**, *132* (17), 6154–6164. (c) Grzegorczyk, W. J.; Savenije, T. J.; Dykstra, T. E.; Piris, J.; Schins, J. M.; Siebbeles, L. D. A. *J. Phys. Chem. C* **2010**, *114*, 5182–5186. (d) Lee, J.; Vandewal, K.; Yost, S. R.; Bahlke, M. E.; Goris, L.; Baldo, M. A.; Manca, J. V.; Van Voorhis, T. *J. Am. Chem. Soc.* **2010**, *132* (34), 11878–11880. (e) Hwang, I. W.; Moses, D.; Heeger, A. J. *J. Phys. Chem. C* **2008**, *112* (11), 4350–4354. (f) Howard, I. A.; Mauer, R.; Meister, M.; Laquai, F. *J. Am. Chem. Soc.* **2010**, *132* (42), 14866–14876.

(4) De, S.; Pascher, T.; Maiti, M.; Jespersen, K. G.; Kesti, T.; Zhang, F. L.; Inganas, O.; Yartsev, A.; Sundstrom, V. *J. Am. Chem. Soc.* **2007**, *129* (27), 8466–8472.

(5) Hodgkiss, J. M.; Campbell, A. R.; Marsh, R. A.; Rao, A.; Albert-Seifried, S.; Friend, R. H. *Phys. Rev. Lett.* **2010**, *104*, 17.

(6) (a) Clarke, T. M.; Ballantyne, A. M.; Nelson, J.; Bradley, D. D. C.; Durrant, J. R. *Adv. Funct. Mater.* **2008**, *18* (24), 4029–4035. (b) Kim, Y.; Cook, S.; Tuladhar, S. M.; Choulis, S. A.; Nelson, J.; Durrant, J. R.; Bradley, D. D. C.; Giles, M.; McCulloch, I.; Ha, C. S.; Ree, M. *Nat. Mater.* **2006**, *5* (3), 197–203.

(7) Nelson, J. *Phys. Rev. B* **2003**, *67* (15), 155209.

(8) Yamamoto, S.; Guo, J.; Ohkita, H.; Ito, S. *Adv. Funct. Mater.* **2008**, *18* (17), 2555–2562.

(9) Theander, M.; Yartsev, A.; Zigmantas, D.; Sundstrom, V.; Mammo, W.; Andersson, M. R.; Inganas, O. *Phys. Rev. B* **2000**, *61* (19), 12957–12963.

(10) Groves, C.; Blakesley, J. C.; Greenham, N. C. *Nano Lett.* **2010**, *10* (3), 1063–1069.

(11) Offermans, T.; Meskers, S. C. J.; Janssen, R. A. *J. Chem. Phys.* **2005**, *308* (1−2), 125–133.

(12) Huang, Y.-S.; Westenhoff, S.; Avilov, I.; Sreearunothai, P.; Hodgkiss, J. M.; Deleener, C.; Friend, R. H.; Beljonne, D. *Nat. Mater.* **2008**, *7* (6), 483–489.

(13) MacKenzie, R. C. I.; Kirchartz, T.; Dibb, G. F. A.; Nelson, J. *J. Phys. Chem. C* **2011**, *115* (19), 9806–9813.

(14) (a) Tachiya, M.; Mozumder, A. *Chem. Phys. Lett.* **1975**, *34* (1), 77–79. (b) Tachiya, M.; Seki, K. *Appl. Phys. Lett.* **2009**, *94* (8), 081104. (c) Hayer, A.; Bassler, H.; Falk, B.; Schrader, S. *J. Phys. Chem. A* **2002**, *106* (46), 11045–11053. (d) Paquin, F.; Latini, G.; Sakowicz, M.; Karsenti, P.-L.; Wang, L.; Beljonne, D.; Stingelin, S.; Silva, C. *Phys. Rev. Lett.* **2011**in press.

(15) (a) Ferenczi, T. A. M.; Nelson, J.; Belton, C.; Ballantyne, A. M.; Campoy-Quiles, M.; Braun, F. M.; Bradley, D. D. C. *J. Phys.: Condens. Matter* **2008**, *20*, 47. (b) Kroeze, J. E.; Savenije, T. J.; Vermeulen, M. J. W.; Warman, J. M. *J. Phys. Chem. B* **2003**, *107* (31), 7696–7705.

(16) Kirkpatrick, J. Covariant Representations of Subproduct Systems, 2010. http://arxiv.org/abs/1004.0344v1.

(17) Swinnen, A.; Haeldermans, I.; vande Ven, M.; D'Haen, J.; Vanhoyland, G.; Aresu, S.; D'Olieslaeger, M.; Manca, J. *Adv. Funct. Mater.* **2006**, *16* (6), 760–765.

(18) Muller, C.; Ferenczi, T. A. M.; Campoy-Quiles, M.; Frost, J. M.; Bradley, D. D. C.; Smith, P.; Stingelin-Stutzmann, N.; Nelson, J. *Adv. Mater.* **2008**, *20* (18), 3510.

(19) Keivanidis, P. E.; Bruno, A.; Nelson, J.; Yartsev, A.; Sundstrom, V. 2011, to be submitted for publication.

(20) Li, G.; Shrotriya, V.; Huang, J. S.; Yao, Y.; Moriarty, T.; Emery, K.; Yang, Y. *Nat. Mater.* **2005**, *4* (11), 864–868.

(21) Peet, J.; Kim, J. Y.; Coates, N. E.; Ma, W. L.; Moses, D.; Heeger, A. J.; Bazan, G. C. *Nat. Mater.* **2007**, *6* (7), 497–500.

(22) (a) Bu, L. J.; Guo, X. Y.; Yu, B.; Qu, Y.; Xie, Z. Y.; Yan, D. H.; Geng, Y. H.; Wang, F. S. *J. Am. Chem. Soc.* **2009**, *131* (37), 13242. (b) King, S.; Sommer, M.; Huettner, S.; Thelakkat, M.; Haque, S. A. *J. Mater. Chem.* **2009**, *19* (30), 5436–5441.

(23) Foster, S.; Finlayson, C. E.; Keivanidis, P. E.; Huang, Y. S.; Hwang, I.; Friend, R. H.; Otten, M. B. J.; Lu, L. P.; Schwartz, E.; Nolte, R. J. M.; Rowan, A. E. *Macromolecules* **2009**, *42* (6), 2023–2030.